

Adjoint “quarks” on coarse anisotropic lattices: Implications for string breaking in full QCD

Karn Kallio and Howard D. Trottier

Physics Department, Simon Fraser University, Burnaby, B.C., Canada V5A 1S6

Abstract

A detailed study is made of four dimensional SU(2) gauge theory with static adjoint “quarks” in the context of string breaking. A tadpole-improved action is used to do simulations on lattices with coarse spatial spacings a_s , allowing the static potential to be probed at large separations at a dramatically reduced computational cost. Highly anisotropic lattices are used, with fine temporal spacings a_t , in order to assess the behavior of the time-dependent effective potentials. The lattice spacings are determined from the potentials for quarks in the fundamental representation. Simulations of the Wilson loop in the adjoint representation are done, and the energies of magnetic and electric “gluelumps” (adjoint quark-gluon bound states) are calculated, which set the energy scale for string breaking. Correlators of gauge-fixed static quark propagators, without a connecting string of spatial links, are analyzed. Correlation functions of gluelump pairs are also considered; similar correlators have recently been proposed for observing string breaking in full QCD and other models. A thorough discussion of the relevance of Wilson loops over other operators for studies of string breaking is presented, using the simulation results presented here to support a number of new arguments.

I. INTRODUCTION AND MOTIVATION

Simulations of lattice QCD are increasingly dedicated to the goal of including the effects of sea quarks on many observables. One of the most distinctive signatures of sea quarks should be the elimination of the confining potential between widely separated valence quarks. Quenched simulations have demonstrated that color-electric field lines connecting a static quark and antiquark are squeezed into a narrow tube or “string” [1]. In full QCD however the flux-tube should be unstable against fission at large separations R , where sea quarks should materialize from the vacuum and bind to the heavy quarks to form a pair of color-neutral bound states.

It is perhaps surprising that some controversy persists in the literature as to whether “string breaking” has actually been observed in lattice simulations, and what techniques are required in order to convincingly demonstrate this phenomenon. This is despite extensive large scale simulations in unquenched QCD by several collaborations [2–6]. This problem has come under renewed attack in the last few years with several new viewpoints emerging as to the underlying cause of the difficulty in observing string breaking, and suggestions as

to the optimal approach for resolving this problem [7–15]. These ideas have stimulated new work on string breaking in simulations of full QCD [16–18], and on a number of models that may shed light on string breaking [19–24].

One suggestion to arise in the literature is that the Wilson loop operator, which has typically been used to study the static potential between heavy quarks, has a very small overlap with the true ground state of the system at large R , and hence is not suited to studies of string breaking [3,7,10]. This has led to the consideration of other operators to study string breaking between static quarks, especially operators that explicitly generate light valence quarks at the positions of the heavy quarks [11,12]. We note that another distinguishing feature of the operators proposed in Refs. [11,12] is that they generate correlation functions which receive disconnected contributions, where a pair of heavy-light bound states propagate independently of one another.

Another point of view was raised by one of us in Ref. [13], where it was suggested that string breaking can indeed be seen using Wilson loops, but that it is essential to propagate the trial states over Euclidean times T of about 1 fm, the characteristic scale associated with hadronic binding. In contrast, typical studies of the static potential in unquenched QCD have been done on lattices with relatively “fine” spacings, limiting the propagation times to well under 1 fm, due to the high computational overhead. The use of coarse lattices enables much more efficient simulations of the static potential at the large scales relevant to string breaking. This was demonstrated in Ref. [13] where an improved action was used to observe string breaking on coarse lattices, using Wilson loops in unquenched QCD in three dimensions, at dramatically reduced computational cost.

In this paper we consider a number of the issues raised in the recent literature on string breaking, by doing simulations of quenched lattice QCD with valence “quarks” in the adjoint representation of the color group. There is a long history of lattice simulations of QCD with adjoint matter fields, which exhibits much of the physics of confinement of real QCD, and which also has a connection to supersymmetric physics [25]. In particular an analogue of string breaking should occur in this model. For instance, the confining flux-tube between a pair of heavy adjoint quarks should be unstable against fission at large R , where gluons can materialize from the sea to bind to the heavy quarks, forming a pair of color-neutral bound states dubbed “gluelumps” [25]. Hence the potential $V_{\text{adj}}(R)$ between a pair of static adjoint quarks in quenched QCD should approach a constant at large R

$$V_{\text{adj}}(R \rightarrow \infty) = 2M_{Qg}, \tag{1}$$

where M_{Qg} is the energy of the lightest gluelump. Once again, despite much effort [25–30,23], string breaking using Wilson loops has not been seen in this model. However it has been suggested very recently that string breaking for adjoint quarks can be seen using correlators that explicitly generate valence gluons [20–22].

Here we undertake a detailed study of four dimensional SU(2) gauge theory with static adjoint quarks (this work was reported in unpublished form in Ref. [31]). We use a tadpole-improved gluon action to do simulations on lattices with coarse spatial spacings a_s . We use highly anisotropic lattices, with fine “temporal” spacings a_t , in order to make a careful study of the time-dependent effective potentials. One lattice used here has $a_s = 0.36$ fm and $a_t = 0.10$ fm, which provides an increase in computational efficiency of some two orders of magnitude compared to simulations of adjoint quarks that were done in Ref. [22] using an

unimproved action on lattices with spacings of about 0.1 fm.

The lattice spacings are first determined from the potentials for quarks in the fundamental representation. We then study the Wilson loop in the adjoint representation, and the masses of magnetic and electric gluelumps, which set the energy scale for string breaking according to Eq. (1). We consider correlators of gauge-fixed static quark propagators, without the string of spatial links that is found in the Wilson loop; this is similar to correlators proposed in Refs. [8,9] as alternatives to the Wilson loop for observing string breaking. We also consider correlation functions for a pair of gluelumps, corresponding to states that explicitly contain valence gluons.

We find that adjoint quark string breaking is extremely difficult to observe using Wilson loops, because of a very strong suppression of the signal, due to approximate Casimir scaling of the static potential. Despite the considerable computational advantage provided by using coarse lattices, we are limited to propagation times well below 1 fm. It is clear from our results that plateaus in the effective mass plots cannot be established at such short times. However it is also clear than a progressive “flattening” of the adjoint potential occurs as the propagation time is increased.

By contrast saturation is readily observed in the effective potential naively constructed from the gluelump-pair correlator. Similar results for some of the observables studied here were recently obtained on “fine” lattices using unimproved actions [20–22]. The adjoint quark results in Refs. [20–22] were interpreted as providing support for the picture [3,7,10] that Wilson loops are not suitable for studies of string breaking, while suggesting that string breaking can readily be observed using operators that explicitly generate states containing light valence particles [11,12].

However we suggest instead that one must be more careful in defining the goal of “observing string breaking” in Euclidean time correlation functions. In particular we note that operators which explicitly generate light valence quarks, such as proposed in Refs. [11,12,20–22], will *automatically* exhibit potentials that saturate, even in *quenched* QCD (here considering the theory with fundamental representation quarks). This is especially clear when the correlator has disconnected contributions. This can also be seen from results presented in Ref. [19], where correlation functions of exactly this form were studied in quenched QCD with fundamental representation quarks. If one goal of string breaking studies is to observe a distinctive feature of the effects of sea quarks, then clearly one must use an observable that distinguishes between the quenched and unquenched theories.

We further argue that using an operator such as the Wilson loop (which might be thought of as creating “initial” states containing only heavy valence quarks) is well motivated by making an analogy with the process of hadronization, which is the physical process that is most often alluded to in the context of “string breaking.” In hadronization the initial state consists of just two valence quarks at small separations, which then separate in real time, leading to the creation of light valence quarks at separations around 1–2 fm. The small overlap of the Wilson loop with the broken string state at much larger separations may be an irreducible feature of using Euclidean time correlators to mimic hadronization; a nonlocal state of two widely separated heavy quarks connected by a string is bound to have a small overlap with the state consisting of two widely separated heavy-light mesons. On the other hand, we find that the overlap of the Wilson loop with the broken string state is appreciable in a range of separations around the point at which string breaking actually

occurs. Simulations of Wilson loops at very large separations, where the overlap becomes very small, are not relevant to hadronization, since in this physical process the original quarks never get to such points with the string intact.

If one considers the static potential for quark separations around 1–2 fm, which are physically motivated by the analogy with hadronization, then “string breaking” does indeed appear to be accessible in full QCD using Wilson loops. The important observation here is that propagation times of about 1 fm must be attained in order to resolve the broken string state [13]. This can be more readily achieved by using improved actions to do simulations on coarse lattices; we estimate that an increase in computational efficiency of some two orders of magnitude over most recent studies in full QCD can reasonably be achieved. This viewpoint is also supported by the results presented here, given the behavior of the time dependent effective masses, even though actual string breaking in adjoint Wilson loops is not resolved. In this connection, we draw attention below to the somewhat surprising fact that string breaking in quenched QCD with adjoint quarks actually has a *much* higher computational burden than in unquenched QCD with real quarks. In our estimation all of the evidence supports the view that string breaking is accessible in large scale simulations of the Wilson loop in full QCD.

The rest of this paper is organized as follows. In Sect. II we present the details of the improved gluon action, and the construction of the various correlation functions to be studied. The results of the simulations are presented in Sect. III, where each correlator is considered in turn. Finally, we present some further discussion and conclusions in Sect. IV.

II. ACTION AND OBSERVABLES

The tadpole-improved SU(2) action on anisotropic lattices used here was previously studied in Ref. [32], following earlier work in SU(3) color [33,34]

$$\begin{aligned} \mathcal{S} = & -\beta \sum_{x, s > s'} \xi_0 \left\{ \frac{5}{3} \frac{P_{ss'}}{u_s^4} - \frac{1}{12} \frac{R_{ss'}}{u_s^6} - \frac{1}{12} \frac{R_{s's}}{u_s^6} \right\} \\ & -\beta \sum_{x, s} \frac{1}{\xi_0} \left\{ \frac{4}{3} \frac{P_{st}}{u_s^2 u_t^2} - \frac{1}{12} \frac{R_{st}}{u_s^4 u_t^2} \right\}, \end{aligned} \quad (2)$$

where $P_{\mu\nu}$ is one half the trace of the 1×1 Wilson loop in the $\mu \times \nu$ plane, $R_{\mu\nu}$ is one half the trace of the 2×1 rectangle in the $\mu \times \nu$ plane, and where ξ_0 is the bare lattice anisotropy,

$$\xi_0 = \left(\frac{a_t}{a_s} \right)_{\text{bare}}. \quad (3)$$

This action has rectangles $R_{ss'}$ and R_{st} that extend at most one lattice spacing in the time direction. This has the advantage of eliminating a negative residue high energy pole in the gluon propagator that would be present if R_{ts} rectangles were included. “Diagonal” correlation functions computed from this action thus decrease monotonically with time, which is very important for our purposes. The leading discretization errors in this action are thus of $O(a_t^2)$ and $O(\alpha_s a_s^2)$.

On an anisotropic lattice one has two mean fields u_t and u_s . Here we define the mean fields using the measured values of the average plaquettes. Since the lattice spacings a_t in our simulations are small, we adopt the following prescription [32–34] for the mean fields

$$u_t \equiv 1, \quad u_s = \langle P_{ss'} \rangle^{1/4}. \quad (4)$$

Observables in various representations of the gauge group can be easily computed from the measured values of the fundamental representation link variables using relations amongst the group characters. The Wilson loop W_j in the j -th representation is defined by

$$W_j \equiv \frac{1}{2j+1} \text{Tr} \left\{ \prod_{l \in L} \mathcal{D}_j[U_l] \right\}, \quad (5)$$

where $\mathcal{D}_j[U_l]$ is the j -representation of the link U_l , and L denotes the path of links in the Wilson loop. In the case of the adjoint Wilson loop of interest here, we have

$$W_1(T, R) = \frac{1}{3} \left(4 |W_{1/2}(T, R)|^2 - 1 \right), \quad (6)$$

as can also be seen by using an explicit form for the adjoint representation matrices [25]

$$\mathcal{D}_1^{ab}[U] = \frac{1}{2} \text{Tr}(\sigma^a U \sigma^b U^\dagger), \quad (7)$$

and making use of the identity $\sigma_{ij}^a \sigma_{kl}^a = 2(\delta_{il}\delta_{jk} - \frac{1}{2}\delta_{ij}\delta_{kl})$.

To enhance the signal-to-noise we make an analytical integration on time-like links [35]

$$\int d[U_l] \mathcal{D}_j[U_l] e^{-\beta S} = \frac{I_{2j+1}(\beta k_l)}{I_1(\beta k_l)} \mathcal{D}_j[V_l] \int d[U_l] e^{-\beta S} \quad (8)$$

where $k_l V_l$ denotes the sum of the 1×1 staples and 2×1 rectangles connected to the time-like link U_l [$\det(V_l) \equiv 1$]. This variance reduction was applied to time-like links for the Wilson loops and gluelump correlators. Equation (8) assumes that a given link appears linearly in the observable, hence we can only apply it to Wilson loops with $R > 2$, because of the rectangles R_{st} that appear in the improved action.

An iterative fuzzing procedure [36] was used to increase the overlap of the Wilson loop and gluelump operators with the lowest-lying states. Fuzzy link variables $U_i^{(n)}(x)$ at the n th step of the iteration were obtained from a linear combination of the link and surrounding staples from the previous step

$$U_i^{(n)}(x) = U_i^{(n-1)}(x) + \epsilon \sum_{j \neq \pm i} U_j^{(n-1)}(x) U_i^{(n-1)}(x + \hat{j}) U_j^{(n-1)\dagger}(x + \hat{i}), \quad (9)$$

where i and j are purely spatial indices, and where the links were normalized to $U^\dagger U = I$ after each iteration. Operators were constructed by using the fuzzy spatial link variables in place of the original links. Typically the number of iterations n and the parameter ϵ were chosen around $(n, \epsilon) = (10, 0.04)$ for Wilson loops and $(n, \epsilon) = (4, 0.1)$ for gluelumps.

The gauge-invariant propagator $G(T)$ of a gluelump can be constructed by coupling a static quark propagator Q_T (product of temporal links) of time-extent T to spatial plaquettes U_0 and U_T located at the temporal ends of the line [25]

$$G(T) = \text{Tr} \left(U_0 \sigma^b \right) \mathcal{D}_1^{ab} [Q_T] \text{Tr} \left(U_T^\dagger \sigma^b \right). \quad (10)$$

Both magnetic and electric gluelump propagators were analyzed, by choosing appropriate linear combinations of spatial plaquettes at the ends of the static propagator [25]. For

the magnetic gluelump a sum of four plaquettes in a particular spatial plane is used, the sum being invariant under lattice rotations about an axis perpendicular the plane. For the electric gluelump a sum of eight plaquettes lying in two planes is used, the sum being invariant under rotations about an axis that lies in both planes. $G(T)$ can be expressed in terms of fundamental representation link variables using Eq. (7)

$$G(T) = 2\text{Tr} \left(U_0 Q_T U_T^\dagger Q_T^\dagger \right) - \text{Tr} (U_0) \text{Tr} (U_T). \quad (11)$$

We also study the correlation between two gluelump propagators, measuring the expectation value of the operator

$$G_{GG}(T, R) \equiv G^\dagger(T; R)G(T; 0), \quad (12)$$

where static quark propagators $Q_{T;0}$ and $Q_{T;R}$ of time-extent T , and separated by a spatial distance R , are used in $G(T; 0)$ and $G(T; R)$, respectively. We also compute the off-diagonal entries in the gluelump pair-Wilson loop mixing matrix, given by the expectation value of the operators

$$G_{GW}(T, R) \equiv \text{Tr} (U_{0;0} \sigma^a) \mathcal{D}_1^{ab} \left[Q_{T;0} \Gamma_{T;R} Q_{T;R}^\dagger \right] \text{Tr} (U_{0;R} \sigma^b), \quad (13)$$

and

$$G_{WG}(T, R) \equiv \text{Tr} (U_{T;R} \sigma^b) \mathcal{D}_1^{ab} \left[Q_{T;R}^\dagger \Gamma_{0;R}^\dagger Q_{T;0} \right] \text{Tr} (U_{T;0} \sigma^b). \quad (14)$$

$\Gamma_{0;R}$ and $\Gamma_{T;R}$ are products of (fuzzy) links connecting the spatial sites of the heavy quarks at times zero and T respectively. The plaquettes $U_{0;0}$ and $U_{0;R}$ in the case of G_{GW} for example are connected to the ends of the static propagators at time zero.

Finally, as an alternative to the Wilson loop, we compute correlators of gauge-fixed static quark propagators separated by a distance R , given by expectation values of the operator

$$G_{\text{Poly}}(T, R) = \text{Tr} (\mathcal{D}_1[Q_{T;0}]) \text{Tr} (\mathcal{D}_1[Q_{T;R}]). \quad (15)$$

This operator is similar to the Wilson loop in that it has only heavy quark propagators. It has been suggested [8,9] that this type of operator may have a larger overlap with the broken string state, since it does not have an explicit string of spatial links connecting the heavy quarks, unlike the Wilson loop. We measured G_{Poly} in lattice Coulomb gauge, where $\sum_{i=1}^3 [U_i(x) - U_i(x - \hat{i})] = 0$, which we implemented using an iterative steepest ascent algorithm with fast Fourier acceleration [37].

III. RESULTS

A. Lattice parameters and fundamental representation potentials

Four lattices were studied in order to check the physical results for dependence on lattice spacing and input anisotropy. The four sets of simulation parameters are listed in Table I. Roughly 40,000 measurements were made for the observables on all lattices, skipping 10 configurations between measurements (which results in very small autocorrelation times).

β	ξ_0	u_s	Volume	ξ_{ren}/ξ_0	a_s (fm)	a_t (fm)	$\Delta V(\sqrt{3}a_s)$
0.848	0.276	0.7933	$10^3 \times 20$	1.02(1)	0.361(8)	0.102(2)	0.078(2)
0.848	0.125	0.8432	$8^3 \times 30$	1.17(1)	0.494(20)	0.072(3)	0.154(2)
0.600	0.125	0.7947	$8^3 \times 30$	1.14(2)	0.606(40)	0.086(6)	0.220(2)
0.500	0.125	0.7648	$8^3 \times 30$	1.12(1)	0.689(30)	0.096(4)	0.231(2)

TABLE I. Simulation parameters for the four lattices, and measured values of some lattice quantities. The bare anisotropies ξ_0 and the mean fields u_s for tadpole improvement are shown (where $u_t \equiv 1$), along with the lattice volume in each case. Measured values of the lattice anisotropies ξ_{ren} are compared to the input anisotropies, as discussed in the text. Simulation results for the spatial and temporal spacings a_s and a_t are given, as well as the relative errors ΔV in the off-axis potentials at $R = \sqrt{3}a_s$.

We note that lattices with coarse spatial spacings a_s were deliberately chosen, in an effort to probe the potentials at the longest physical quark separations possible, for the least computational cost. Lattice spacings around 0.4 fm have been studied by a number of authors (see e.g. Refs. [38,34,32]). Using the lattice with $a_s = 0.36$ fm here provides an increase in computational efficiency of some two orders of magnitude compared to the simulations of adjoint quarks done on lattices with “fine” spacings in Ref. [22]. Still coarser spacings were also considered here and, although one would not necessarily advocate the use of such lattices for precision calculations, it is worthwhile to employ them in an effort to glean some information about string breaking, where much remains to be understood.

We first present results for the fundamental representation Wilson loop, which are used to measure the renormalized lattice anisotropy ξ_{ren} and to set the lattice spacing a_s . These results demonstrate fairly good scaling and rotational symmetry restoration, as well as fairly small renormalizations of the input anisotropy, thanks to the tadpole improvement of the action.

The renormalized anisotropy is determined by comparing the static potential $a_t V_{xt}$, computed in units of a_t from Wilson loops W_{xt} where the time axis is taken in the direction of small lattice spacings, with the potential $a_s V_{xy}$ computed from Wilson loops W_{xy} with both axes taken in the direction of large lattice spacings [32–34,39]. The anisotropy is determined after an unphysical constant is removed from the potentials, by subtraction of the simulation results at two different radii

$$\xi_{\text{ren}} = \frac{a_t V_{xt}(R_2) - a_t V_{xt}(R_1)}{a_s V_{xy}(R_2) - a_s V_{xy}(R_1)}. \quad (16)$$

The anisotropies determined with $R_1 = \sqrt{2}a_s$ and $R_2 = 2a_s$ are shown in Table I; results obtained with $R_1 = a_s$ are in excellent agreement with these estimates. The renormalization of the anisotropy is fairly small in all cases, especially as compared to the very large renormalizations for unimproved actions on lattices with comparable spacings [32].

The spatial lattice spacing is then determined by fitting the fundamental representation potential to the form

$$V_{\text{fit}}(R) = \sigma R - \frac{b}{R} + c, \quad (17)$$

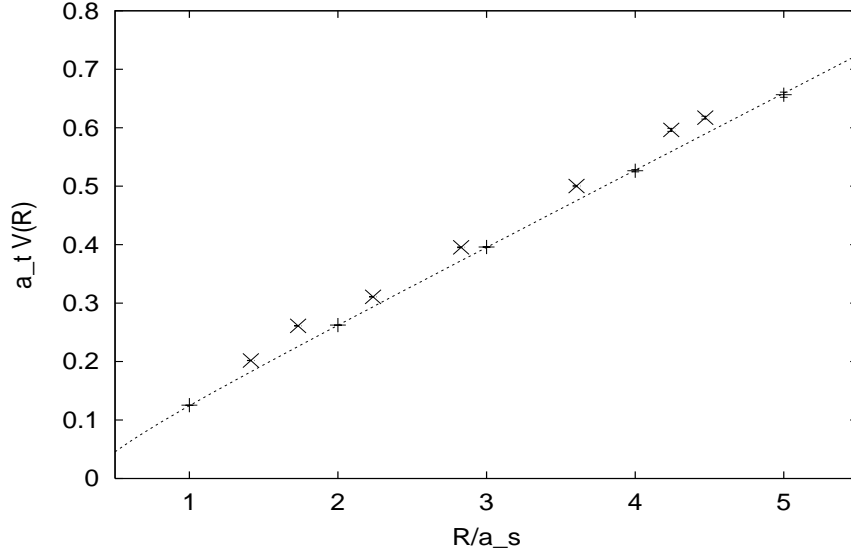


FIG. 1. Fundamental representation potential for the action with $a_s = 0.49$ fm: on-axis points (+), off-axis points (\times). The dotted line shows the results of a fit of the on-axis points to Eq. (17).

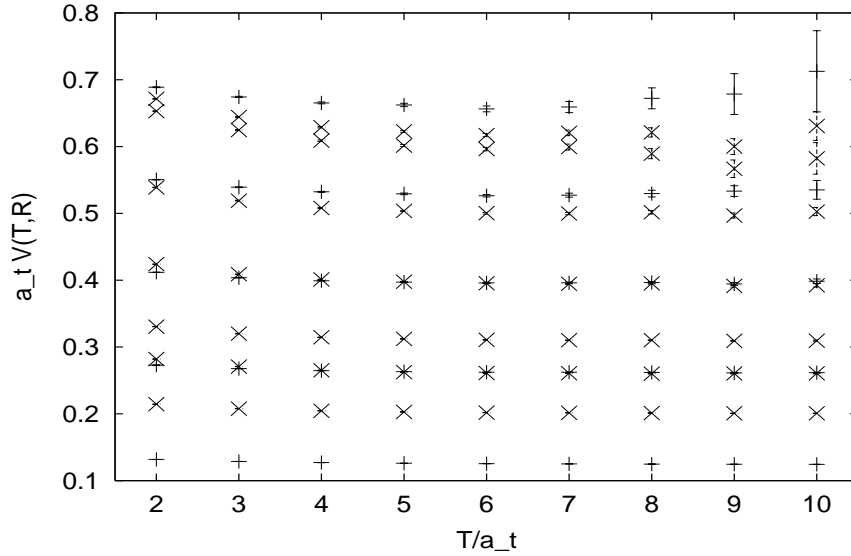


FIG. 2. Time-dependent effective mass plot for the fundamental potential from the lattice with $a_s = 0.49$ fm and $a_t = 0.072$ fm. Each roughly horizontal line of points shows the effective mass at one separation R : on-axis points (+), off-axis points (\times).

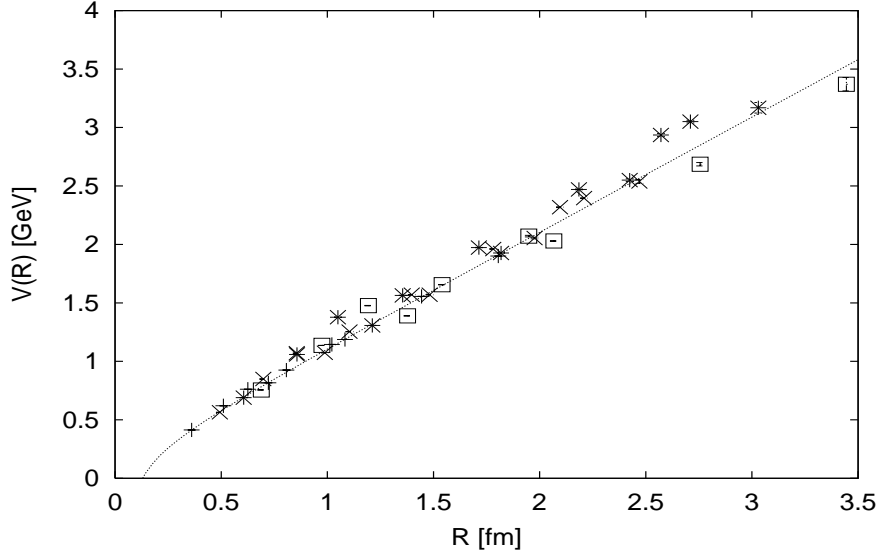


FIG. 3. Fundamental representation potentials in physical units from all four lattices: $a_s = 0.36$ fm (+), $a_s = 0.49$ fm (\times), $a_s = 0.61$ fm (*), and $a_s = 0.69$ fm (\square). An additive renormalization in the energies has been adjusted so that the potentials agree at $R \approx 0.5$ fm. The dotted line is the best fit to Eq. (17) for the lattice with $a_s = 0.36$ fm.

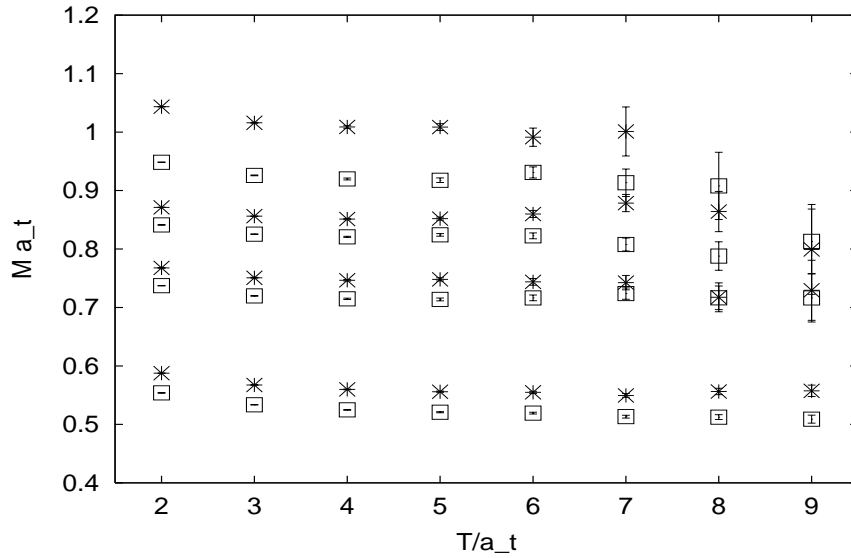


FIG. 4. Effective mass plots for single electric (*) and magnetic (\square) gluelumps. There are four pairs of plots corresponding to the four lattices, with the spatial spacing a_s increasing from the bottom of the figure to the top.

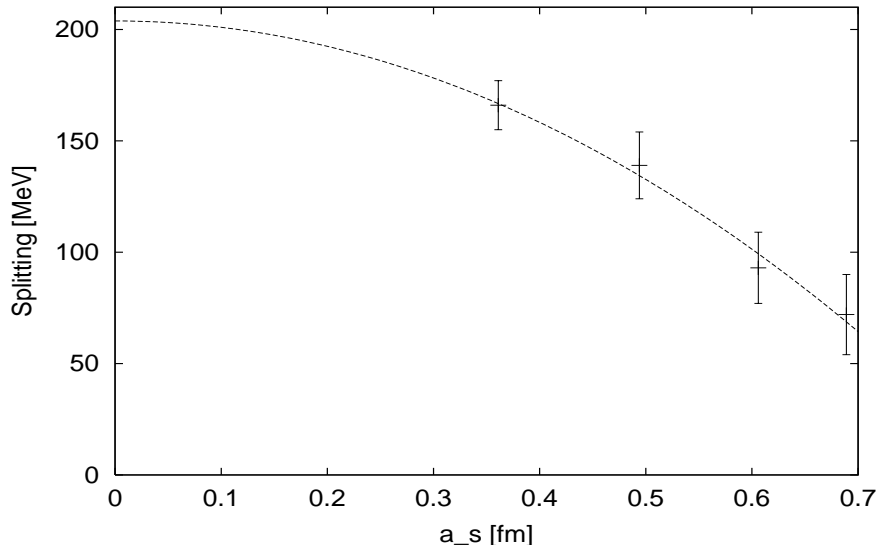


FIG. 5. Gluelump physical mass splitting versus lattice spacing a_s . The dashed curve shows a fit assuming $O(a^2)$ scaling violations.

taking the physical value of the string tension to be $\sqrt{\sigma} = 0.44$ GeV. The potentials were measured at on-axis separations, as well as at off-axis separations $R/a_s = \sqrt{2}, \sqrt{3}, \sqrt{5}, \sqrt{8}, \sqrt{13}, \sqrt{18},$ and $\sqrt{20}$. Symmetric combinations of the shortest spatial paths connecting two lattice points were used in the nonplanar Wilson loop calculations. Results for the lattice with $a_s = 0.49$ fm are given in Fig. 1, which shows fairly good rotational symmetry restoration, thanks to tadpole improvement. A quantitative measure of the symmetry breaking is obtained by comparing the simulation results for the potential with the interpolation to the on-axis data

$$\Delta V(R) \equiv \frac{V_{\text{sim}}(R) - V_{\text{fit}}(R)}{\sigma R}. \quad (18)$$

Results for ΔV at $R = \sqrt{3}a_s$ for the four lattices are shown in Table I. Unimproved actions exhibit much larger rotational symmetry breaking effects on such coarse lattices [32].

Representative plots of the time-dependent effective potential

$$V(T, R) = -\ln \left(\frac{W(T, R)}{W(T-1, R)} \right) \quad (19)$$

are shown in Fig. 2. A reliable determination of the ground state potential in the fundamental representation can be made, with excellent plateaus in the effective mass plots, going out to propagation times near 1 fm, even at separations as large as 2.5 fm.

The potentials from all four lattices are plotted together in physical units in Fig. 3. A Coulomb term is visible in this data, with fits to the on-axis data yielding coefficients b around 0.1 [32]. Although the fundamental potentials on these coarse lattices are dominated by the confinement term, the results give some indication of fairly good scaling behavior.

B. Magnetic and electric gluelumps

The effective mass plots for single electric and magnetic gluelumps exhibit good plateaus, as shown in Fig. 4. The electric gluelump is known to have the larger mass [25]. The gluelump energy M_{Qg} is not physical as it must be additively renormalized due to the self energy of the heavy quark. However this renormalization should cancel in the difference between the electric and magnetic gluelump energies. A direct comparison of $2M_{Qg}$ with the static potential for a pair of adjoint quarks is also meaningful since the two quantities have equal self energies.

Our results for the gluelump splittings on the four lattices are:

$$M_{\text{elec}} - M_{\text{mag}} = \begin{cases} 166 \pm 11 \text{ MeV}, & a_s = 0.36 \text{ fm}, \\ 139 \pm 15 \text{ MeV}, & a_s = 0.49 \text{ fm}, \\ 93 \pm 16 \text{ MeV}, & a_s = 0.61 \text{ fm}, \\ 72 \pm 18 \text{ MeV}, & a_s = 0.69 \text{ fm}, \end{cases} \quad (20)$$

and are plotted versus lattice spacing in Fig. 5. For the sake of illustration, a fit assuming $O(a^2)$ scaling violations yields a continuum estimate of

$$M_{\text{elec}} - M_{\text{mag}} = (204 \pm 16) \text{ MeV}, \quad \chi^2/\text{dof} = 0.29, \quad (21)$$

while a fit assuming $O(a)$ scaling violations yields

$$M_{\text{elec}} - M_{\text{mag}} = (273 \pm 29) \text{ MeV}, \quad \chi^2/\text{dof} = 0.50. \quad (22)$$

These results are consistent with an estimate of the gluelump splitting in SU(2) color by Jorysz and Michael [25], who found $M_{\text{elec}} - M_{\text{mag}} = 203 \pm 76 \text{ MeV}$, using a single lattice with a spacing of about 0.16 fm.

C. Adjoint representation Wilson loops

The determination of the ground state potential in the adjoint representation is much more difficult than in the fundamental case, due at least in part to a much larger overall energy scale in the adjoint channel. Effective mass plots for the adjoint potential on two lattices are shown in Figs. 6 and 7. Notice that the temporal spacing is smaller in Fig. 7, allowing one to more clearly see that plateaus in the effective masses at large separations have not been reached. The trend in the effective mass plots at large R is not inconsistent with the suggestion [13] that string breaking occurs at propagation times of about 1 fm.

A typical procedure followed in the literature on string breaking is to estimate the ground state potential $V(R)$ as equal to the effective potential $V(T, R)$ at a small value of T , especially at large R , given the poor signal-to-noise in this region. The effect of choosing different fixed values of T for the determination of the potential can be seen by plotting $V(T, R)$ versus R , for several choices of T . We show our data in this way for one lattice in Fig. 8. There is a clear trend for the “potential” to flatten as T is increased, and this trend continues until the signal at large R is lost in the noise. The limitation to such small propagation times $T \lesssim 0.4 \text{ fm}$ at large separations introduces a significant systematic error in assessing whether the potential saturates.

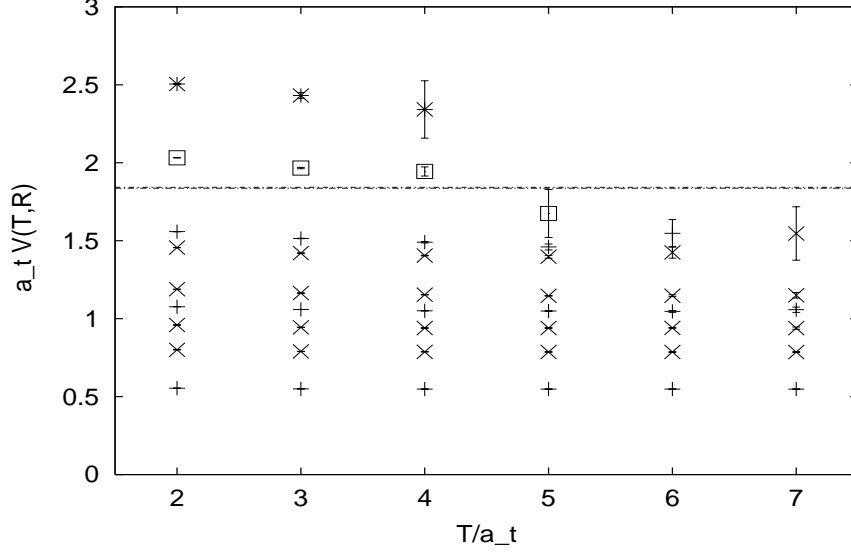


FIG. 6. Adjoint Wilson loop effective mass plots for the lattice with $a_s = 0.36$ fm and $a_t = 0.10$ fm. Plots are shown for several values of the on-axis quark separation, $R = 1-3$ (+), $R = 4$ (\square) and $R = 5$ (*), as well as at some off-axis points (\times). The dashed lines show the 1σ limits for twice the mass of the magnetic gluelump $2M_{Qg}$ on this lattice.

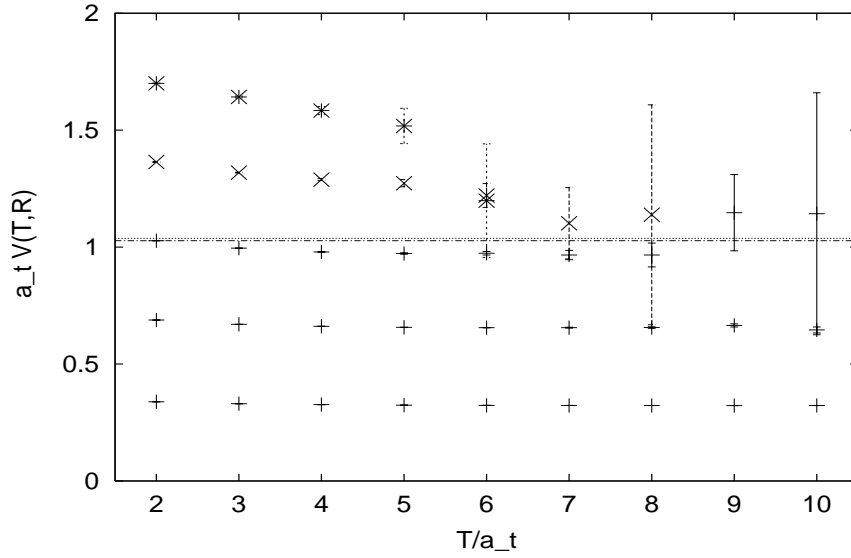


FIG. 7. Adjoint Wilson loop effective mass plots for the lattice with $a_s = 0.49$ fm and $a_t = 0.072$ fm. Plots are shown for $R = 1-3$ (+), $R = 4$ (\times), $R = 5$ (*).

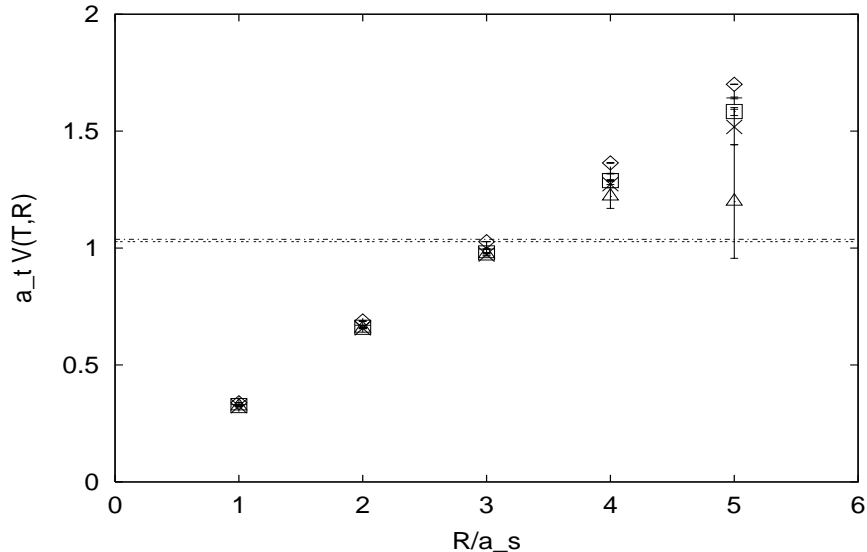


FIG. 8. Adjoint Wilson loop static potential vs R at various fixed propagation times, for the lattice with $a_s = 0.49$ fm and $a_t = 0.07$ fm: $T/a_t = 2$ (\diamond), 3 ($+$), 4 (\square), 5 (\times), 6 (\triangle). The dotted lines show 1σ limits for $2M_{Qg}$ (magnetic).

It is also useful to compare the fundamental potential with the adjoint one. In Fig. 9 we plot the two potentials in physical units from all four lattices, where we rescale the adjoint potential by $3/8$, the ratio of $SU(2)$ Casimirs for the two representations. There is good evidence for screening of the adjoint potential, compared to simple models of Casimir scaling [25], but again the extent of the screening (or possible saturation) cannot be reliably determined, due to the limitation to short propagation times.

D. Gauge-fixed quark-antiquark correlator

The correlation function between a pair of static adjoint quark propagators (cf. Eq. (15)) was calculated in Coulomb gauge, in order to study a state without an explicit string of links connecting the heavy quarks. Similar correlators were suggested for observing string breaking in Refs. [8,9]. Results for the effective potential defined from $G_{\text{Poly}}(T, R)$ are shown for one lattice in Fig. 10. The results obtained from this correlator agree well with the Wilson loop estimate of the potential, obtained at similar propagation times, giving neither a better nor a worse indication of string breaking.

E. Gluelump-gluelump correlators

Representative effective mass plots for the magnetic gluelump-gluelump correlator (cf. Eq. (12)) for one lattice are shown in Fig. 11. At smaller separations the signal is clear but contains large excited state contributions; at larger separations the signal degrades, but the data at small T show more of a plateau. The resulting potentials from two lattices are compared in physical units in Fig. 12.

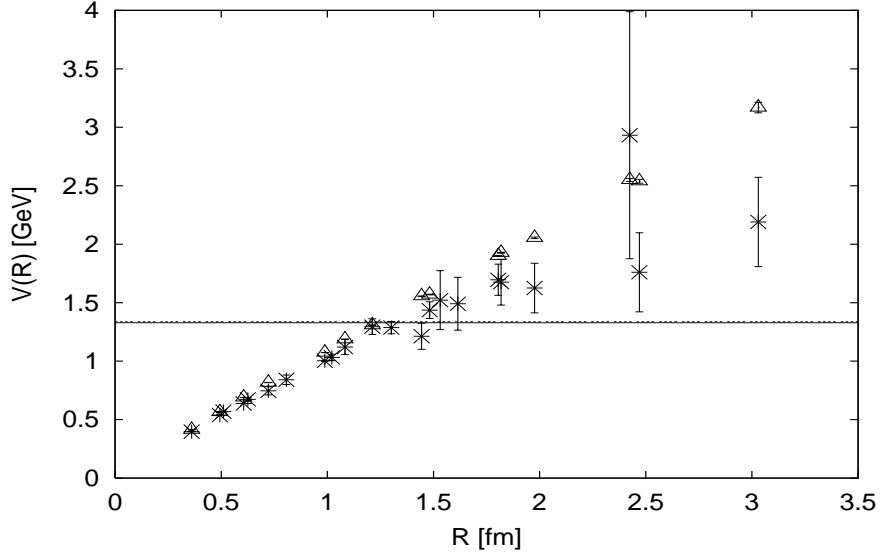


FIG. 9. Comparison of the adjoint (*) and fundamental (Δ) potentials in physical units from all four lattices. The adjoint potential has been multiplied by a factor of $3/8$ and shifted vertically to agree with the fundamental potential at $R \approx 0.5$ fm. The dashed lines show 1σ limits for $2M_{Qg}$ (magnetic), after being rescaled and shifted vertically by the same amount as the adjoint potential (here using the results only at $a_s = 0.36$ fm).

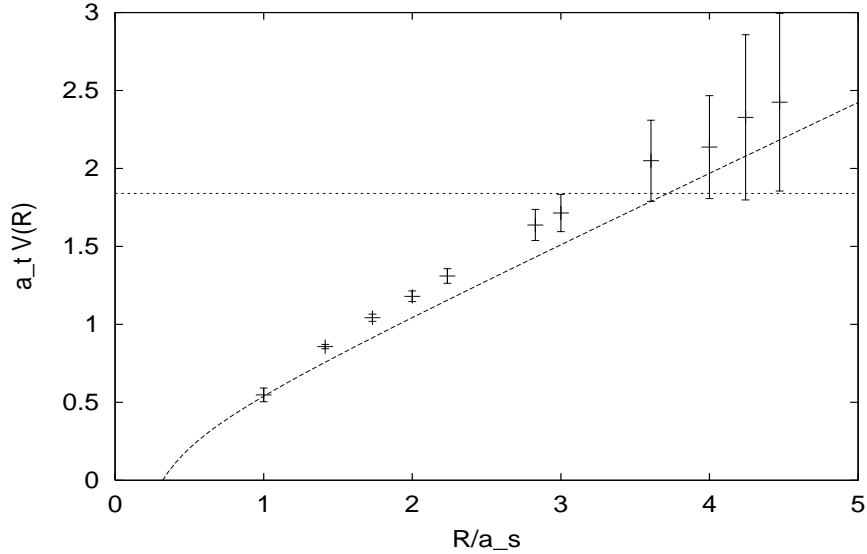


FIG. 10. Adjoint potential computed from gauge-fixed static quark propagators on the lattice with $a_s = 0.36$ fm and $a_t = 0.10$ fm. The dotted line shows $2M_{Qg}$ (magnetic), and the dashed curve shows the result of a fit to the potential computed from the adjoint Wilson loop on the same lattice and at comparable propagation times.

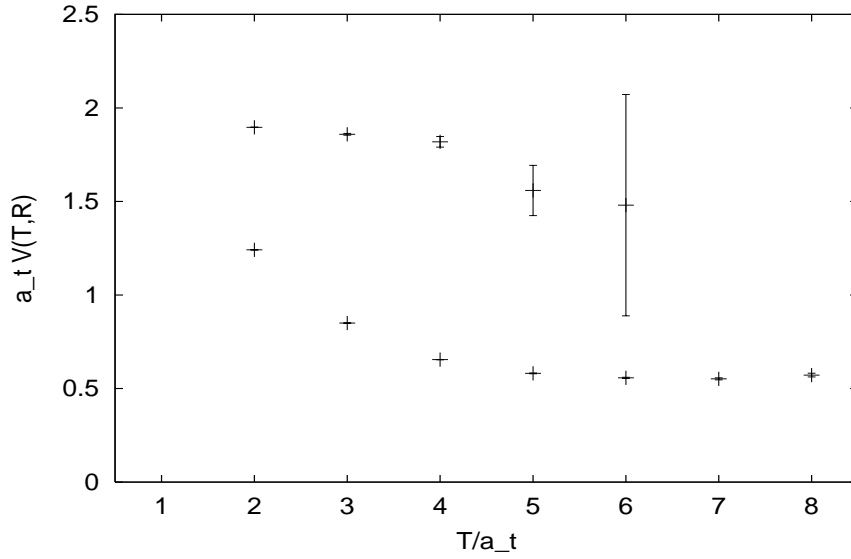


FIG. 11. Magnetic gluelump-gluelump effective masses for the lattice with $a_s = 0.36$ fm and $a_t = 0.10$ fm, for two separations: $R = 1$ (lower points) and $R = 4$ (upper points).

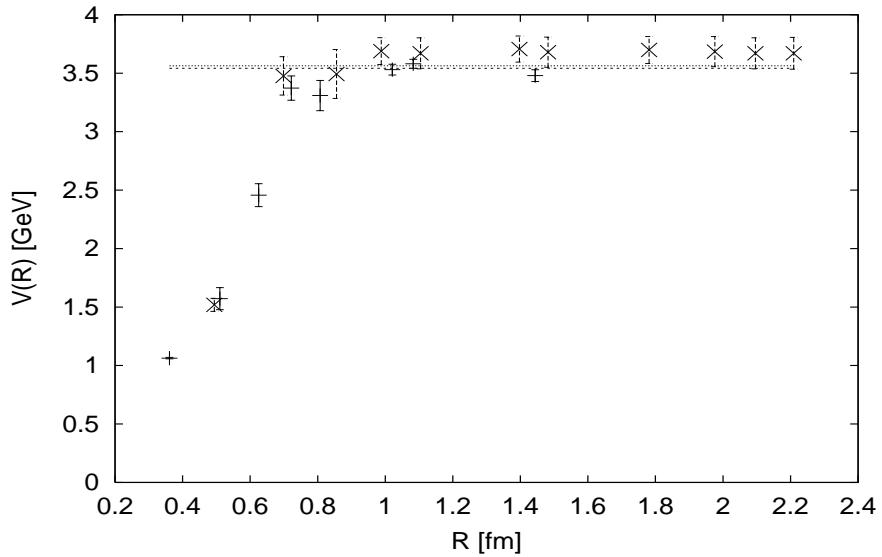


FIG. 12. Static potential estimates from the magnetic gluelump-pair correlator in physical units (with additive energy shifts): $a_s = 0.36$ fm (+) and $a_s = 0.49$ fm (\times).

We also used a standard variational method [25] to estimate the state of lowest energy in the 2×2 basis of states composed of a pair of heavy adjoint quarks connected to each other by a string of links (adjoint Wilson loop W_{adj}), and a pair of gluelumps. Consider the corresponding 2×2 correlation matrix C_{ij} (cf. Eqs. (12)–(14))

$$C_{ij}(T, R) = \begin{pmatrix} \langle W_{\text{adj}}(T, R) \rangle & \langle G_{GW}(T, R) \rangle \\ \langle G_{WG}(T, R) \rangle & \langle G_{GG}(T, R) \rangle \end{pmatrix}. \quad (23)$$

Representing the two basis states by $|\phi_i(R)\rangle$, the correlation matrix $C_{ij}(T, R)$ is written as a transfer matrix

$$C_{ij}(T, R) = \langle \phi_i(R) | e^{-HT} | \phi_j(R) \rangle. \quad (24)$$

We first find a linear combination $|\Phi(R)\rangle$ of basis states

$$|\Phi(R)\rangle = \sum_i a_i(R) |\phi_i(R)\rangle \quad (25)$$

which maximizes

$$\lambda(T^*, R) = \frac{\langle \Phi(R) | e^{-HT^*} | \Phi(R) \rangle}{\langle \Phi(R) | \Phi(R) \rangle}. \quad (26)$$

This requires the solution of the eigenvalue problem

$$C_{ij}(T^*, R) a_j(R) - \lambda(T^*, R) C_{ij}(0, R) a_j(R) = 0. \quad (27)$$

We choose to optimize the variational state by solving Eq. (27) at a small time T^* , otherwise numerical instabilities may arise due to large statistical errors in $C_{ij}(T^*, R)$, especially at large R .

We then evolve the correlation function Eq. (26) for the variational state to a larger time T , in order to filter out our final estimate of the ground state energy $\lambda(T, R) = e^{-E_0(R)T}$. The overlaps $c_i^2(R) = \langle \phi_i(R) | \mathcal{O}(R) \rangle^2 / \langle \phi_i(R) | \phi_i(R) \rangle$ of the basis states $|\phi_i(R)\rangle$ on the ground state $|\mathcal{O}(R)\rangle$ can be estimated according to

$$c_i^2(R) = \frac{C_{ii}(T, R)}{\lambda(T, R) C_{ii}(0, R)}, \quad (28)$$

at sufficiently large T (Eq. (28) at finite T provides an upper bound on the overlaps).

The results of this diagonalization procedure are as might be expected. Figure 13 shows the estimate of the ground state potential in physical units from two lattices. The estimated overlaps of the Wilson loop and gluelump-pair states with the variational estimate of the ground state are shown in Fig. 14. There is a rapid cross-over in the ground state as determined in this basis, from the Wilson loop at smaller R to the gluelump-pair state at larger R . The rapid cross-over suggests that the gluelump-pair state becomes dominated by disconnected contributions when the energies of the states near $2M_{Qg}$.

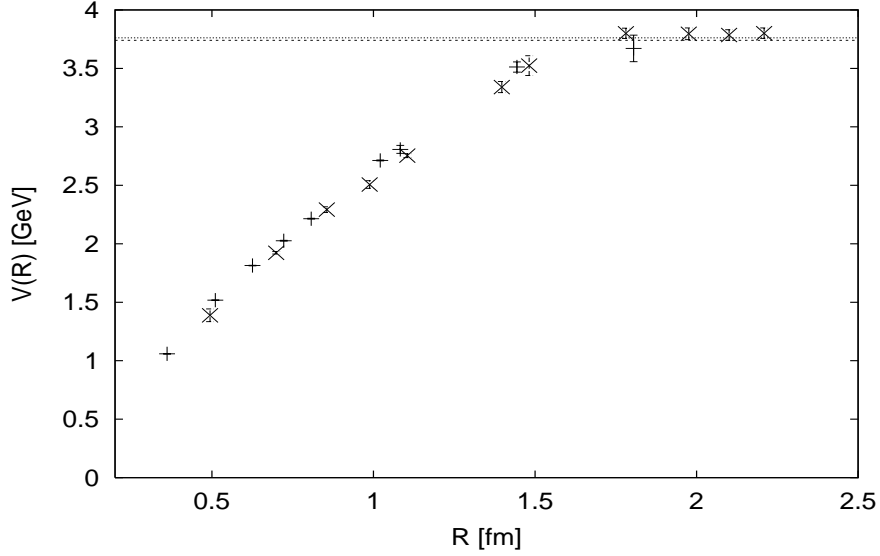


FIG. 13. Variational estimate of the ground state energy in physical units for two lattices (after additive shifts in the energies): $a_s = 0.36$ fm (+) and $a_s = 0.49$ fm (\times). The trial state was typically determined at $T^* = a_t$, which was then propagated to a time $T \approx 4a_t$ to obtain the results shown in the figure. Also shown are the 1σ lines for $2M_{Qg}$ (magnetic).

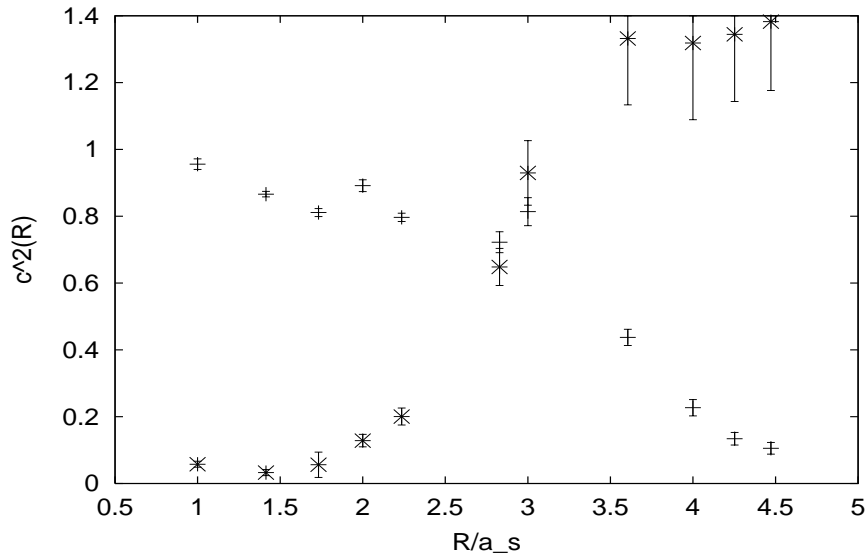


FIG. 14. Diagonalization results for the lattice with $a_s = 0.49$ fm, showing the overlaps of the two basis states with the ground state as functions of R , estimated from Eq. (28): Wilson loop (+) and gluelump-pair (*).

IV. SUMMARY AND FURTHER DISCUSSION

In this paper we made a through analysis of adjoint quark physics in the context of string breaking. Three trial states were investigated as candidates for observing string breaking: the adjoint Wilson loop, a pair of gluelump propagators, and a pair of gauge-fixed static quark propagators. The fundamental representation potentials were used to measure the lattice parameters, and electric and magnetic gluelump masses were calculated in order to set the energy scale for string breaking. A number of techniques were used to maximize the efficiency of the calculations, including fuzzing, variance reduction, and fast Fourier accelerated gauge fixing. Particularly important was the use of coarse, highly anisotropic lattices from tadpole-improved actions. The lattice with $a_s = 0.36$ fm and $a_t = 0.10$ fm for example gives an improvement in computational efficiency of some two orders of magnitude compared to simulations of adjoint quarks done in Ref. [22] on lattices with spacings of about 0.1 fm. Large lattice anisotropies provided more data points for analysis of the Euclidean time evolution of correlation functions. This proved to be especially important in analyzing adjoint Wilson loops for even moderate physical values of R , due to the rapid decay of the signal.

Diagonalization in a two state basis, corresponding to adjoint Wilson loops and the gluelump-pair operators, reveals a static potential which saturates at $2M_{Qg}$ near 1.5 fm. Similar string breaking distances have been suggested for full QCD [40], and have been observed in other theories, including three-dimensional QCD with dynamical fermions [13]. At small quark separations the potential rises linearly, with a slope of about $\frac{8}{3}$ of the fundamental potential, consistent with Casimir scaling. Saturation in the potential obtained from the diagonalization occurs over a very small range of separations R . These results are in qualitative agreement with recent calculations done on fine lattices using unimproved actions [20–22]. In addition, results obtained here using correlations between gauge-fixed static quark propagators agree well with the Wilson loop estimate of the potential, giving neither a better nor a worse indication of string breaking.

As discussed in Sect. I these results, taken at face value, might be interpreted as evidence that Wilson loops are not suitable for studies of string breaking, and that string breaking can be readily observed using operators that explicitly contain fields for the light particles. However we raised several cautionary observations about this viewpoint. In particular, we pointed out in Sect. I that operators which explicitly generate a pair of light valence particles *automatically* exhibit potentials that saturate. In the case of QCD with fundamental representation quarks, this means that operators of this type would demonstrate “string breaking” even in the quenched theory. This is particularly clear when the correlation function receives disconnected contributions. In the case of the gluelump-pair correlator (cf. Eq. (12)), we have

$$\langle 0|G^\dagger(T; R)G(T; 0)|0\rangle = \langle 0|G(T; 0)|0\rangle^2 + \dots, \quad (29)$$

where $|0\rangle$ is the vacuum state, and where the ellipsis denotes the contributions of non-vacuum insertions between the two operators in the correlator. Hence one is guaranteed to find an effective mass of $2M_{Qg}$ at modest R using this correlation function. This also helps to explain the rapid cross-over that is observed in variational calculations using Wilson loops and such states [11,12,20–22], when the energies of the states approach the broken string energy.

Exactly the same behavior must occur if operators that explicitly generate light valence quarks are used in simulations of QCD with fundamental representation quarks. This can also be seen from some recent work using such operators in quenched QCD [19]. Thus operators of the type that have recently been proposed in Refs. [11,12] for observing string breaking will yield qualitatively the same behavior in both quenched and unquenched QCD.

This raises the important question of exactly how one defines the goal of “observing string breaking.” Perhaps one can advocate two points of view. From one point of view, one would say that correlation functions give spectral information only: the ground state energy versus quark separation. In this view such information is useful, for example, in characterizing the effects of quenching on meson-meson interaction energies [41,42], but not in relation to processes such as hadronization, which can only occur in the presence of dynamical fermions. Then one might say that the difficulty in seeing “string breaking” with the Wilson loop at very large separations indicates nothing more than that this operator has a poor overlap with the ground state in this regime. If spectral information is all that one is interested in, then one might not be too concerned that a particular operator shows qualitatively similar behaviour in the quenched and unquenched theories.

A second point of view, which we raised in Sect. I, is that one can use certain correlation functions to make an analogy with hadronization. One might argue that this may be done by considering operators that do not generate light valence particles in the trial state. In particular, the operator should exhibit “string breaking” only in unquenched QCD (here considering the theory with fundamental representation quarks). The Wilson loop is such an operator, while operators which explicitly generate light valence particles are not. Moreover, if a goal of string breaking studies is to observe a distinctive feature of the effects of sea quarks, then one should only consider observables that distinguish between the quenched and unquenched theories. In a sense the first point of view discussed above is concerned with “static” spectral information, that is qualitatively similar in the quenched and unquenched theories, while the second point of view makes contact with a “dynamical” process that is unique to the unquenched theory.

In making contact with hadronization one is interested in using the Wilson loop to measure the potential for separations R not much larger than the distance at which the string breaks, $R \approx 1.5$ fm, since in the actual physical process the original quarks never get to larger separations with the string intact. In this region the overlap of the Wilson loop with the ground state appears to be appreciable, judging from Fig. 14, and from results presented in Ref. [13]. However one must still push the calculation to propagation times of about 1 fm, in order to properly resolve the broken string. This is where the difficulty actually lies in observing string breaking using Wilson loops.

To date most simulations of full QCD have been done on lattices with relatively fine spacings, making it computationally very challenging to reach the length scales $R \approx 1.5$ fm and propagation times $T \approx 1$ fm relevant to string breaking. The use of coarse lattices with improved actions allows a much more efficient probe of this regime, as was recently demonstrated by one of us in Ref. [13], where this approach was used to resolve string breaking with Wilson loops in unquenched QCD in three dimensions. An increase in computational efficiency of some two orders of magnitude is possible using lattices with spacings between 0.3 fm and 0.4 fm, compared to most simulations that have been done so far in unquenched QCD. Some work in this direction has recently been reported in Ref. [17].

Unfortunately calculations of the adjoint Wilson loop in this string breaking regime did not prove to be feasible in this paper, with propagation times limited to well below 1 fm, even with coarse lattices. On the other hand it is clear that adjoint Wilson loops exhibit a potential that progressively “flattens” at longer propagation times. Moreover, the trend in the effective mass plots from the adjoint Wilson loop at large R is not inconsistent with the suggestion that string breaking would be observed at propagation times of about 1 fm.

In this context it is interesting to estimate the size of the adjoint Wilson loop signal relative to the fundamental one, and to compare the computational cost of these simulations to those of unquenched QCD. If we assume roughly Casimir scaling of the potential just below the string breaking distance, then the ratio $W_{\text{adj}}/W_{\text{fund}}$ of the adjoint to the fundamental Wilson loops in SU(3) color goes like

$$W_{\text{adj}}/W_{\text{fund}} \approx \exp \left[-\left(\frac{9}{4} - 1\right)\sigma RT \right] \approx 10^{-4}, \quad (30)$$

using $\sqrt{\sigma} = 0.44$ GeV for the fundamental representation string tension, and $R \approx 1.5$ fm and $T \approx 1$ fm for the scales relevant to string breaking (the ratio is yet smaller, by an order of magnitude, in SU(2) color). This is to be compared with the roughly two orders of magnitude increase in the cost of simulating dynamical quarks compared to quenched simulations. (Note that the gluelump-gluelump correlator [20–22] does not show a comparable suppression of the signal, which is entirely a consequence of not removing the disconnected contributions from the correlator). Hence, while the adjoint representation is interesting as a probe of confinement and supersymmetric physics, it is not a cost effective means of mimicking hadronization in full QCD.

On the other hand the results presented here do lend support to the general picture that Wilson loops should in fact exhibit “string breaking,” as an analogy to hadronization. Moreover string breaking should be accessible in real QCD with the computational power currently available in large scale simulation environments, especially if coarse lattices with improved actions are used.

ACKNOWLEDGMENTS

We thank E. Eichten, B. Jennings, J. Juge, G. Moore and R. Woloshyn for fruitful conversations. This work was supported in part by the Natural Sciences and Engineering Research Council of Canada.

REFERENCES

- [1] For a review see C. Michael, Report No. hep-ph/9710249.
- [2] U. Glassner *et al.*, SESAM Collaboration, Phys. Lett. B **383**, 98 (1996).
- [3] S. Aoki *et al.*, CP-PACS collaboration, Nucl. Phys. (Proc. Suppl.) **73**, 216 (1999).
- [4] M. Talevi *et al.*, UKQCD Collaboration, Nucl. Phys. (Proc. Suppl.) **63**, 227 (1998).
- [5] G. Bali *et al.*, SESAM and T χ L collaborations, Nucl. Phys. B (Proc. Suppl.) **63**, 209 (1998).
- [6] C.R. Allton *et al.*, UKQCD Collaboration, Phys. Rev. D **60**, 034507 (1999); J. Garden, hep-lat/9909066.
- [7] S. Güsken, Nucl. Phys. B (Proc. Suppl.) **63**, 16 (1998).
- [8] W. Bürger *et al.*, Nucl. Phys. (Proc. Suppl.) B **30**, 729 (1993).
- [9] C. DeTar *et al.*, Phys. Rev. D **59**, 031501 (1999).
- [10] I. T. Drummond, Phys. Lett. B **434**, 92 (1998). I. T. Drummond, and R.R. Horgan, Phys. Lett. B **447**, 298 (1999).
- [11] O. Philipsen and H. Wittig, Phys. Rev. Lett. **81**, 4056 (1998).
- [12] F. Knechtli and R. Sommer, Phys. Lett. B **440**, 345 (1998);
- [13] H. D. Trottier, Phys. Rev. **60**, 034506 (1999).
- [14] F. Gliozzi and P. Provero, Nucl. Phys. **B556**, 76 (1999).
- [15] For recent reviews of string breaking see, J. Kuti, Nucl. Phys. (Proc. Suppl.) **73**, (1999); K. Schilling, hep-lat/9909152.
- [16] C. DeTar, U. Heller, and P. Lacock, hep-lat/9909078.
- [17] A. Duncan, E. Eichten, and H. Thacker, hep-lat/9909123.
- [18] P. Pennanen and C. Michael, hep-lat/0001015.
- [19] C. Stewart and R. Koniuk, Phys. Rev. D **59**, 114503 (1999).
- [20] P. W. Stephenson, Nucl. Phys. **B550**, 427 (1999).
- [21] O. Philipsen and H. Wittig, Phys. Lett. B **451**, 146 (1999).
- [22] P. de Forcrand and O. Philipsen, hep-lat/9912050
- [23] S. Deldar, hep-lat/9911008.
- [24] F. D. R. Bonnet *et al.*, hep-lat/9912044.
- [25] C. Michael, Nucl. Phys. **B259**, 58 (1985); L.A. Griffiths, C. Michael, and P.E.L. Rakow, Phys. Lett. B **150**, 196 (1985); N.A. Campbell, I.H. Jorjysz, and C. Michael Phys. Lett. B **167**, 91 (1986); I.H. Jorjysz and C. Michael, Nucl. Phys. **B302**, 448 (1988); C. Michael, Nucl. Phys. B (Proc. Suppl.) **26**, 417 (1992). M. Foster and C. Michael, Phys. Rev. D **59**, 094509 (1999).
- [26] R. D. Mawhinney, Phys. Rev. D **41**, 3209 (1990).
- [27] H. D. Trottier and R. M. Woloshyn, Phys. Rev. D **48**, 2290 (1993).
- [28] H. D. Trottier, Phys. Lett. B **357**, 193 (1995).
- [29] G. I. Poulis and H. D. Trottier, Phys. Lett. B **400**, 358 (1997).
- [30] G. S. Bali, hep-lat/9908021.
- [31] K. Kallio, M.Sc. thesis, Simon Fraser University (1999).
- [32] N. H. Shakespeare and H. D. Trottier, Phys. Rev. D **59**, 014502 (1999).
- [33] M. Alford, T. R. Klassen, G. P. Lepage, C. J. Morningstar, and M. Peardon (unpublished).
- [34] C. J. Morningstar, Nucl. Phys. B (Proc. Suppl.) **53**, 914 (1997); C. J. Morningstar and M. Peardon, Phys. Rev. D **56**, 4043 (1997).

- [35] G. Parisi, R. Petronzio, and F. Rapuano, *Phys. Lett. B* **126**, 250 (1983).
- [36] M. Albanese *et al.*, *Phys. Lett. B* **192**, 163 (1987).
- [37] C. T. H. Davies *et al.*, *Phys. Rev. D* **41**, 1953 (1990).
- [38] M. Alford, W. Dimm, G. P. Lepage, G. Hockney, and P. B. Mackenzie, *Nucl. Phys. B (Proc. Suppl.)* **42**, 787 (1995); *Phys. Lett. B* **361**, 87 (1995).
- [39] T. R. Klassen, *Nucl. Phys.* **B533**, 557 (1998).
- [40] C. Alexandrou *et al.*, *Nucl. Phys. B* **414**, 815 (1994).
- [41] C. Stewart and R. Koniuk, *Phys. Rev. D* **57**, 5581 (1998).
- [42] A. Mihaly *et al.*, *Phys. Rev. D* **55**, 3077 (1997).